

# Phase-Shifted Long-Period Fiber Gratings based on Electric-Arc Discharges

Rosane Falate, Orlando Frazão, Gaspar Rego, José L. Fabris, and José L. Santos

**Abstract**—In this work, we present phase-shifted long-period gratings based on the electric-arc technique. Our produced gratings were analyzed with different physical parameters: refractive index, temperature, and strain. Linear responses are obtained for strain sensitivity and non-linear responses for refractive index and temperature changes.

**Index Terms**—Electric-arc discharge, Long-period fiber gratings, Optical fiber devices, Phase-shift gratings

## I. INTRODUCTION

A long-period fiber grating (LPFG) is a periodic modulation of the refractive index of a single-mode optical fiber. This periodic modulation (normally from 100  $\mu\text{m}$  to 800  $\mu\text{m}$ ) couples light from the guided fundamental mode to the forward propagating cladding modes of an optical fiber [1].

LPFG are commonly fabricated by exposure of an optical fiber to UV laser radiation through an amplitude mask [1]. This writing process needs the fiber to be hydrogen loaded in order to enhance the change in the refractive index and usually also requires post-thermal annealing for stabilizing the grating. Two techniques that surpass these pre- and post-fabrication care are the writing processes relying on the exposure of standard fibers to an infrared  $\text{CO}_2$  laser radiation [2] or to electric-arc discharges [3].

When two long-period fiber gratings are fabricated near each other one of two different situations occurs: cascaded long-period fiber gratings and phase-shifted long-period fiber gratings [4]–[7]. The first device is similar to a Mach-Zehnder

interferometer with the two gratings acting as two couplers and the guided and cladding modes in the fiber between them acting as the two arms in the interferometer. The phase delay, which occurs between the light propagating along the core and the cladding of the fiber along the separation of the two gratings, is wavelength dependent and the transmission spectrum is modulated with multiple peaks [7]. The second device occurs when the distances between the fibers are enough small that the phase delay becomes a phase-shift. In such case, when a phase-shift of  $\pi$  is introduced at the center of the grating, the conventional minimum of LPFG becomes a maximum and two new rejection bands appear. This is the result of converting destructive interference into constructive interference at the phase-matching wavelength because of the introduction of the  $\pi$  phase shift at the center [5].

In 1997, Bakhi *et al* demonstrated the first  $\pi$  phase-shifted long-period fiber grating [6]. In such case, to produce the grating they used a specific amplitude-mask with a half missing period in the center and ultraviolet laser illumination. Humbert and Malki [8] have used the advantages of the electric-arc discharge writing process to produce the PS-LPFG. This process, which the fiber does not need to be hydrogen loaded, forms the grating step-by-step and the introduction of any phase-shift is simply performed by translating the fiber by a distance  $L_p$  equivalent to the required phase-shift.

In this work, PS-LPFG based on electric-arc discharges is used to investigate its sensitivity when different physical parameters are applied to it. Linear and nonlinear responses for wavelength shift were obtained.

## II. PHASE-SHIFTED LONG-PERIOD GRATING FABRICATION

The phase-shifted long-period gratings were written in Corning SMF-28 fiber using the electric-arc discharge technique [3]. The fabrication process consists in placing an uncoated fiber between the electrodes of a fusion splice machine. One end of the fiber is clamped in a holder on top of a motorized translation stage controlled with a precision of 0.1  $\mu\text{m}$ . At the other end a weight is attached to keep the fiber under a constant axial tension. An arc discharge is then produced with an electric current of 8.5–10.0 mA during 0.5–2.0 s exposing a short length of the fiber. After the discharge, the translation stage (computer controlled) displaces the fiber by a distance that represents the grating period ( $\Lambda$ ), typically 400–700  $\mu\text{m}$ , several times ( $N$ ) until a required attenuation

Manuscript received June 15, 2005. This work was supported in part by the CAPES under Grant BEX: 0301/04-3, CNPq (Brazilian Agencies) and INESC Porto. G. Rego is also thankful for the grant conceded by the Program PRODEF III.

R. Falate is with Unidade de Optoelectrónica e Sistemas Electrónicos do INESC Porto, 4169-007 Porto, Portugal, and also with Centro Federal de Educação Tecnológica do Paraná, Curitiba-PR, CEP. 80230-901 Brazil. (corresponding author to provide phone: 351-22-6082601; fax: 351-22-6082799; e-mail: rfalate@yahoo.com).

O. Frazão, G. Rego, and J. L. Santos are with Unidade de Optoelectrónica e Sistemas Electrónicos do INESC Porto, 4169-007 Porto, Portugal. (corresponding author to provide phone: 351-22-6082601; fax: 351-22-6082799).

G. Rego is also with Escola Superior de Tecnologia e Gestão, IPVC, Av. do Atlântico, 4900-348 Viana do Castelo, Portugal.

J. L. Fabris is with Centro Federal de Educação Tecnológica do Paraná, Curitiba-PR, CEP. 80230-901 Brazil (e-mail: fabris@cefetpr.br).

loss-peak is obtained. The gratings spectra were recorded using an optical spectrum analyzer set to a resolution of 1.0 nm, and the illumination being provided by a white light source. Every phase-shifted grating has the following fabrication parameters: weight of 5.1 g, a period of 540  $\mu\text{m}$ , an electric current of 9.5 mA, and an arc duration of 1 s. The location of the phase-shift, which corresponds to a displacement of 118  $\mu\text{m}$ , was determined when the transmission loss at the resonance wavelength is approximately 6.9 dB. The three different gratings used in this work are described in the Table I. The total grating length is given by  $(N-1)*\Lambda+L_p$ .

TABLE I - PHASE-SHIFTED LONG-PERIOD GRATINGS

Name	Number of discharges $N$ (before+phase-shift+after)	Measured parameter
PS-LPFG01	35+1+35 = 71	Refractive index
PS-LPFG02	32+1+32 = 65	Temperature, strain
PS-LPFG03	28+1+28 = 57	Strain, torsion, load

Fig. 1 shows the transmission spectrum of PS-LPFG02 at the point where the grating was stopped to produce the phase-shift (dot line) and at the final written process (solid line). The bandpass (named as PHASE-SHIFT) as a result of the destructive interference and the two lateral reject bands (named LOSS 1 and LOSS 2 for lower and higher wavelengths, respectively) are evident. The insertion losses are estimated to be 0.99 dB at maximum passband.

### III. EXPERIMENTAL RESULTS

In order to investigate the spectral response, the spectra were taken when different physical parameters were applied. The sensitivities were obtained based on the wavelength shift measurement of each phase-shift peak (PHASE-SHIFT, LOSS 1 and LOSS 2), and the best curve fit.

The refractive index measurements were taken using the PS-LPFG01 grating. In this case the optical spectrum analyzer was set to a resolution of 0.1 nm, and an erbium-doped broadband source was used to illuminate the grating.

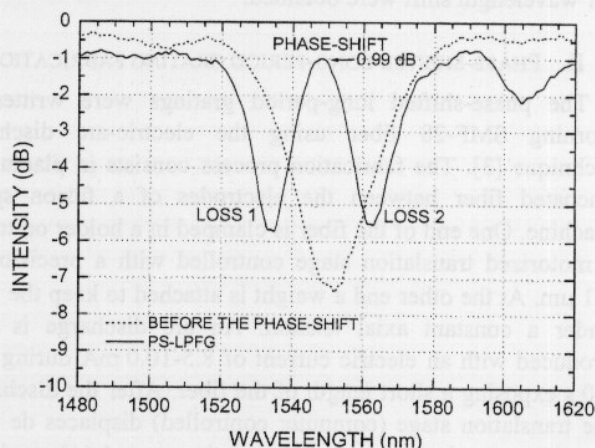


Fig. 1. Transmission spectra of PS-LPFG02 before the phase-shift to be applied (dot line) and at the final written process (solid line).

Fig. 2 shows the wavelength shifts of each phase-shift peak when the external refractive index was changed from 1.333 to 1.428. The refractive indexes of the samples were measured with an Abbe refractometer working at 589 nm. The wavelength shifts, considering the initial wavelength the one obtained for 1.333, were 4.5, 4.8, and 4.9 nm, respectively. For the peaks generated from the phase-shift, this result shows that the longer wavelength resonances have higher refractive index sensitivities than shorter wavelength resonances.

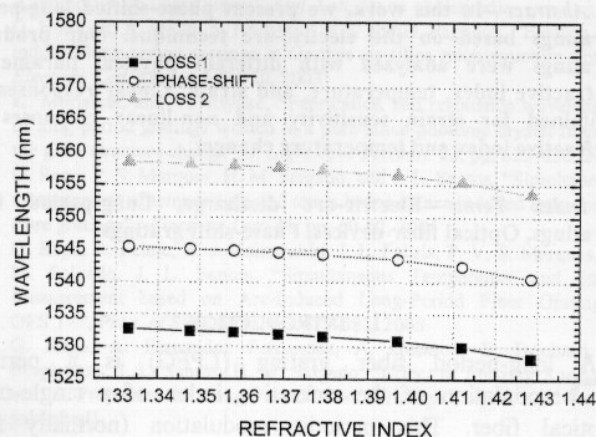


Fig. 2. Wavelength evolutions of PS-LPG01 when external refractive indexes surround the optical fiber. The higher wavelength shift is obtained for LOSS 2.

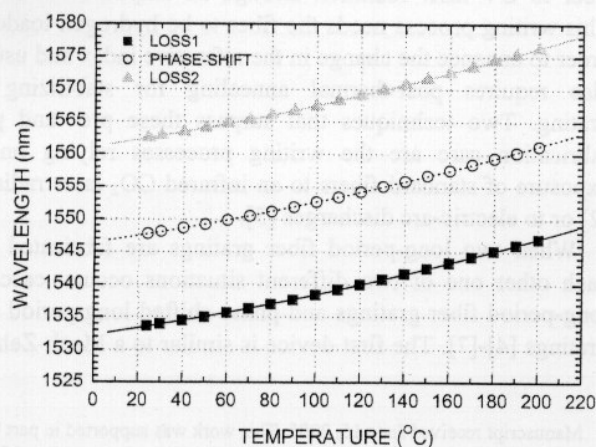


Fig. 3. Temperature response of PS-LPG02.

TABLE II - TEMPERATURE SENSITIVITY OF PS-LPFG02

Name	Linear Fit	Polynomial Fit
LOSS 1 (nm)	$1531.17+0.0764 \cdot T$ $r = 0.99709$	$1532.29+0.0469 \cdot T+1.210 \times 10^{-4} \cdot T^2$ $r = 0.99990$
PHASE-SHIFT (nm)	$1545.29+0.0772 \cdot T$ $r = 0.99718$	$1546.41+0.0505 \cdot T+1.205 \times 10^{-4} \cdot T^2$ $r = 0.99990$
LOSS 2 (nm)	$1559.97+0.0788 \cdot T$ $r = 0.99709$	$1561.14+0.0510 \cdot T+1.254 \times 10^{-4} \cdot T^2$ $r = 0.99995$

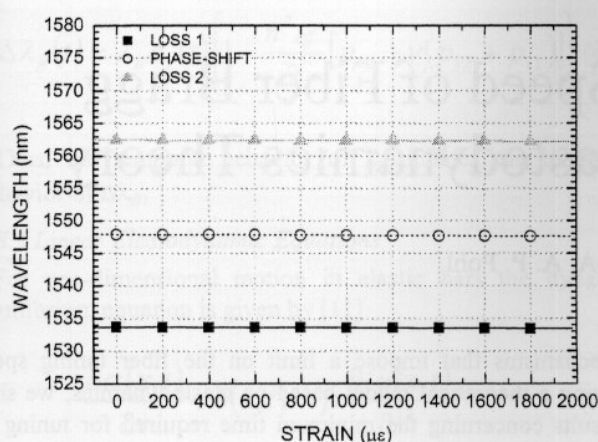


Fig. 4. Strain response of PS-LPG02.

TABLE III - STRAIN SENSITIVITY OF PS-LPFG02

Peak	Strain sensitivity (pm/με)	Correlation coefficient $r$
LOSS 1	-0.141	0.9868
PHASE-SHIFT	-0.170	0.9826
LOSS 2	-0.139	0.9820

TABLE IV - PHASE-SHIFTED LONG-PERIOD GRATING APPLICATIONS

Reference	Application
[5],[7]-[8]	Filter applications based on tailoring the spectral response
[10]	Optical amplifier gain equalizer
[6],[8]	Bandpass and pair of band-rejection filters
[11]	Bandpass filter for actively mode-locked erbium fiber lasers
[12]-[14]	Optical fiber sensors for multi-parameters

For temperature ( $T$ ) and strain ( $S$ ) measurements the same optical spectrum analyzer resolution and source were used, but the grating is the PS-LPFG02. The temperature was changed in the range of 25-200 °C and the result is presented in Fig. 3. The temperature response of the grating is non-linear as can be noticed on Table II, where  $r$  is the correlation coefficient, and agrees with the results obtained by Humbert and Malki [9]. Table II also shows that the longer wavelength resonance has the highest sensitivity when compared with the other two peaks produced with the phase-shift.

Fig. 4 shows the strain sensitivity of PS-LPFG02. The strain sensitivities compared to refractive index and temperature sensitivities are approximately constant. Table III Measurements applying strain, load and torsion to PS-LPFG03 were taken. It was also observed a negligible wavelength shift for these parameters, when compared with refractive index and temperature. This can be expected since the strain sensitivity for this grating was also small (about -0.150 pm/με).

Phase-shifted long-period fiber gratings are interesting for optical communications and sensors applications because they are easy to fabricate, have low back-reflection, and low insertion loss. Table IV shows some applications of phase-shifted long-period fiber gratings.

## IV. CONCLUSION

Phase-shifted long-period fiber gratings using the electric-arc writing process were obtained. Strain sensitivities are linear with the highest value -0.170 pm/με for the bandpass. Temperature and refractive index sensitivities are non-linear and the highest sensitivities for both parameters were obtained for the longest wavelength band rejection when the three peaks generated from the phase-shift are analyzed.

## REFERENCES

- [1] A. M. Vengsarkar, P. J. Lemaire, J. B. Judkins, V. Bhatia, T. Erdogan, and J. E. Sipe, "Long-period fiber gratings as band-rejection filters," *J. Lightwave Technol.*, vol. 14, no. 1, pp. 58-65, Jan 1996.
- [2] D. D. Davis, T. K. Gaylord, E. N. Glytsis, S. G. Kosinski, S. C. Mettler, and A. M. Vengsarkar, "Long-period fiber gratings fabrication with focused CO<sub>2</sub> laser pulses," *Electron. Lett.*, vol. 34, no. 3, pp. 302-303, Feb 1998.
- [3] G. Rego, O. Okhotnikov, E. Dianov, and V. Sulimov, "High-temperature stability of long-period fiber gratings produced using an electric arc," *J. Lightwave Technol.*, vol. 19, no. 10, pp. 1574-1579, Oct 2001.
- [4] E. M. Dianov, S. A. Vasiliev, A. S. Kurkov, O. I. Medvedkov, and V. N. Protopopov, "In-fiber Mach-Zehnder interferometer based on pair of long-period gratings," in *ECOC '96, 22<sup>nd</sup> European Conference on Optical Communication*, 1996, pp. 65-68.
- [5] H. Ke, K. S. Chiang, and J. H. Peng, "Analysis of phase-shifted long-period fiber gratings," *IEEE Photon. Technol. Lett.*, vol. 10, no. 11, pp. 1596-1598, Nov 1998.
- [6] F. Bakhti, and P. Sansonetti, "Realization of low back-reflection, wideband fiber bandpass filters using phase-shifted long-period gratings," in *Tech. Digest OFC'97*, Dallas, TX, USA, 1997, pp. 349-350.
- [7] Y. Liu, J.A.R. Williams, L. Zhang, and I. Bennion, "Phase shifted and cascaded long-period fiber gratings," *Opt. Commun.*, vol. 164, pp. 27-31, Jun 1999.
- [8] G. Humbert, and A. Malki, "High performance bandpass filters based on electric arc-induced  $\pi$ -shifted long-period fibre gratings," *Electron. Lett.*, vol. 39, no. 21, pp. 1506-1507, Oct 2003.
- [9] G. Humbert, and A. Malki, "Electric-arc-induced gratings in non-hydrogenated fibres: fabrication and high-temperature characterizations," *J. Opt. A: Pure Appl. Opt.*, vol. 4, pp. 194-198, Feb 2002.
- [10] J. R. Quian, and H. F. Chern, "Gain flattening fibre filters using phase-shifted long period fibre gratings," *Electron. Lett.*, vol. 34, no. 11, pp. 1132-1133, May 1998.
- [11] O. Deparis *et al.*, "Bandpass filters based on  $\pi$ -shifted long-period fiber gratings for actively mode-locked erbium fiber lasers," *Opt. Lett.*, vol. 26, no. 16, pp. 1239-1241, Aug 2001.
- [12] M. Kong, W. Zhou, and W. Tang, "Optical fiber sensor with phase-shifted long-period fiber gratings," *Proc. SPIE*, vol. 3555, pp. 442-446, Aug 1998.
- [13] Y.-G. Han, W.-T. Han, U.-C. Paek, and Y. Chung, "Measurement of bending curvature using bandpass filters based on phase-shifted long-period fiber gratings," in *Tech. Digest of Optical Fiber Sensor Conference - OFS'2002*, 2002, pp. 143-146.
- [14] Y.-G. Han, J. H. Lee, and S. B. Lee, "Discrimination of bending and temperature sensitivities with phase-shifted long-period fiber gratings depending on initial coupling strength," *Opt. Express*, vol. 12, no. 4, pp. 3204-3208, July 2004.